ADVANCED HEALTHCARE MATERIALS
www.advhealthmat.de

Light-Regulated Angiogenesis via a Phototriggerable VEGF Peptidomimetic

*Roshna V. Nair, Aleeza Farrukh, and Aránzazu del Campo**

The application of growth factor based therapies in regenerative medicine is limited by the high cost, fast degradation kinetics, and the multiple functions of these molecules in the cell, which requires regulated delivery to minimize side effects. Here a photoactivatable peptidomimetic of the vascular endothelial growth factor (VEGF) that allows the light-controlled presentation of angiogenic signals to endothelial cells embedded in hydrogel matrices is presented. A photoresponsive analog of the 15-mer peptidomimetic Ac-KLTWQELYQLKYKGI-NH_2 (abbreviated ^{P}QK) is prepared by introducing a 3-(4,5-dimethoxy-2-nitrophenyl)-2-butyl (DMNPB) photoremovable protecting group at the Trp4 residue. This modification inhibits the angiogenic potential of the peptide temporally. Light exposure of ^{P}QK modified hydrogels provide instructive cues to embedded endothelial cells and promote angiogenesis at the illuminated sites of the 3D culture, with the possibility of spatial control. ^{P}QK modified photoresponsive biomaterials offer an attractive approach for the dosed delivery and spatial control of pro-angiogenic factors to support regulated vascular growth by just using light as an external trigger.

1. Introduction

Angiogenesis or vascularization during tissue repair is typically promoted by providing vascular endothelial growth factor (VEGF) as a soluble factor or bounded to the biomaterial scaffold.[1] VEGF is a large protein and has a short lifetime ($\tau_{1/2}$ of VEGF is 40 min in vitro[2]). This makes VEGF treatments cost-intensive. As a potential solution to the limited stability and high costs of therapeutic VEGF, proangiogenic peptidomimetics have been proposed.[3] Among different variants, the sequence Ac-KLTWQELYQLKYKGI-amide (QK) developed by D'Andrea group in 2005 seems to be the most effective candidate.[3a] This sequence mimics the 17–25 α-helical region of VEGF that binds to VEGF receptors (VEGFRs) (**Figure 1**A,B) and activates VEGFR-2 gene upregulation upon binding.[4] In terms of stability, QK has been found to retain its bioactivity for at least 24 h in 50% human serum, much longer than the 90 min half-life of the full-length VEGF in vivo.[4] Added at a nanomolar concentration to the culture medium, QK promoted proliferation and angiogenic differentiation of endothelial cells (ECs).[3a] QK-mediated microvascularization ex vivo and in vivo[4,5] has been demonstrated.[6,7] Recent reports also support the application of QK to central nervous system (CNS) therapies, as it is shown to permeate the blood-brain barrier.[3b]

For controlled and prolonged delivery, QK has been encapsulated and delivered from different hydrogels,[7] poly(ethylene glycol)-b-poly(L-lactide-co-e-caprolactone) emulsions,[8] and from porous poly-(sulfobetaine methacrylate).[9] Alternatively, controlled presentation of QK has been achieved by attaching the peptide to instructive matrices, and tubulogenesis and endothelial sprouting have been demonstrated.[3b] For this purpose, QK was covalently bound to a collagenase-degradable poly(ethylene glycol) diacrylate matrix,[10] to elastin-like polypeptide hydrogels (10 nM–100 μM QK grafting density),[11] or fused to a collagen-binding peptide and attached to collagen scaffolds[12] and to decellularized extracellular matrix.[13]

The therapeutic window for VEGF treatment is narrow, consequently, low doses are safe but not sufficient to yield a therapeutic benefit, and slightly higher doses lead to the growth of angioma-like vascular structures.[14] Moreover, angiogenesis in vivo requires sustained angiogenic stimulus over a month to achieve stable vessels, and the outcome of the process is highly dependent on the spatial distribution (concentration gradient) of the proangiogenic signal.[15] In recent years photoactivatable peptidomimetics[16] have allowed the regulated presentation of bioactive molecules to cells in engineered hydrogels using light.[17] By attaching photoremovable protecting groups to the side chain of a relevant residue for receptor binding, the affinity of the peptide for binding to the receptor is temporally decreased. Upon light exposure at appropriate wavelength and dose, the photoremovable group is cleaved, the peptidomimetic is activated and cellular processes are triggered.[18] With this approach, spatiotemporal controlled integrin binding and cell

Dr. R. V. Nair, Dr. A. Farrukh, Prof. A. del Campo
INM – Leibniz Institute for New Materials
Saarbrücken 66123, Germany
E-mail: aranzazu.delcampo@leibniz-inm.de
Prof. A. del Campo
Chemistry Department
Saarland University
Saarbrücken 66123, Germany

The ORCID identification number(s) for the author(s) of this article can be found under https://doi.org/10.1002/adhm.202100488

DOI: 10.1002/adhm.202100488

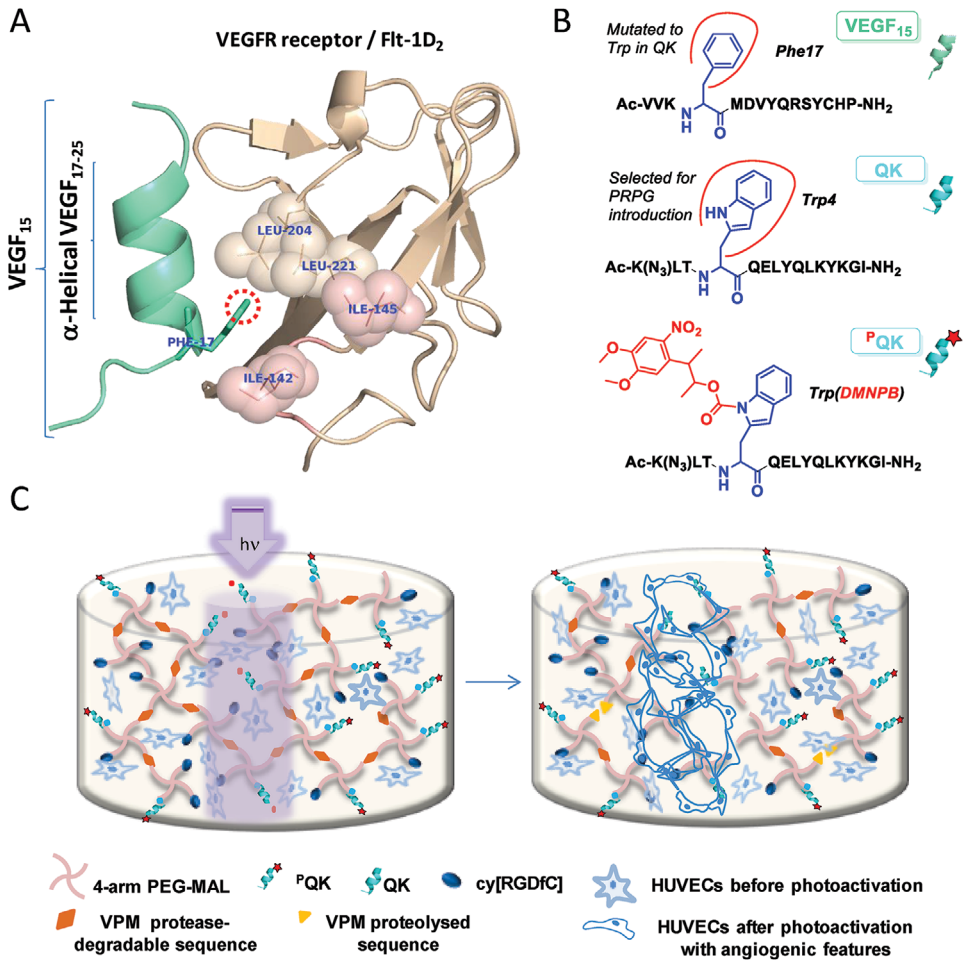

Figure 1. A) Structure of the binding region of the α-helical region of VEGF-A (from which structure of QK was derived) with Flt-1D$_2$ receptor (PDB: FLT1), taken as the basis for the design of ^{P}QK. The interactive region of Phe17 with different residues on the VEGF receptor in domain 2 of Flt-1 is labeled and represented in spheres. Position for the photoremovable protecting group (PRPG) insertion to perturb the binding interactions is represented by the red dotted circle. (NB: For simplification, only a trimmed section of VEGF-A is shown. In PDB: FLT1, two monomers of VEGF$_{8-109}$ are shown sandwiched between two Flt-1D$_2$ domains). B) Peptide sequences of VEGF$_{15}$, QK, and ^{P}QK. C) Scheme showing the spatially localized photoactivation of ^{P}QK/RGD functionalized PEG hydrogels with encapsulated HUVECs and the subsequently activated angiogenesis in the desired space.

adhesion, migration, and differentiation processes have been realized in vitro and in vivo.[19] Recently also light-regulated angiogenesis in a 3D culture was demonstrated via photoactivation of cell adhesive ligands within a hydrogel in the presence of soluble VEGF.[18d] In this work, we present an advanced approach to regulate angiogenesis by functionalizing hydrogels with a photoactivatable derivative of the proangiogenic factor QK (^{P}QK) and regulating its presentation with light (Figure 1C). This strategy avoids the systemic exposure to VEGF doses and facilitates the delivery of the angiogenic signal at localized sites and controlled concentration capable of inducing physiological microvascular networks to support vascular growth.

2. Results and Discussion

2.1. Chemical Design and Synthesis of ^{P}QK

The sequence of the QK peptide Ac-KLTWQELYQLKYKGI-NH$_2$ is based on the modified N-terminal helical region of VEGF-A$_{17-25}$ (VEGF$_{15}$/Ac-VVKF$_{17}$M$_{18}$D$_{19}$VYQRS$_{24}$Y$_{25}$CHP-NH$_2$, synthetic peptide equivalent to the α-helical region of VEGF) (Figure 1B). QK includes a few mutated positions and it conserves the α-helical secondary structure of the native sequence, which has been demonstrated crucial for binding to VEGFRs.[3a] In particular, Phe17 (F17) was replaced by Trp to increase hydrophobic interactions, Met18 by Gln to increase hydrogen bonding interactions at the receptor site, and Asp19 by Glu and Ser24 by Lys to enhance helical propensity. The N- and C-capping acetyl and amide groups were introduced to improve stability.[3a] Helicity of QK allows Trp4 (W4), Tyr8 (Y8), and Tyr12 (Y12) to interact with VEGFR-1D$_2$ predominantly via hydrophobic interactions (Figure 1A). These amino acids are located at a distance <4.5 Å from the surface of the receptor.[20] With this structural information, we hypothesized that the residues Trp4 (W4), Tyr8 (Y8), or Tyr12 (Y12) could be suitable positions to introduce photolabile groups and inhibit the binding interaction of QK with VEGFRs (molecular structure in **Figure S1**, Supporting Information). Previous structure-activity profile studies of QK had revealed

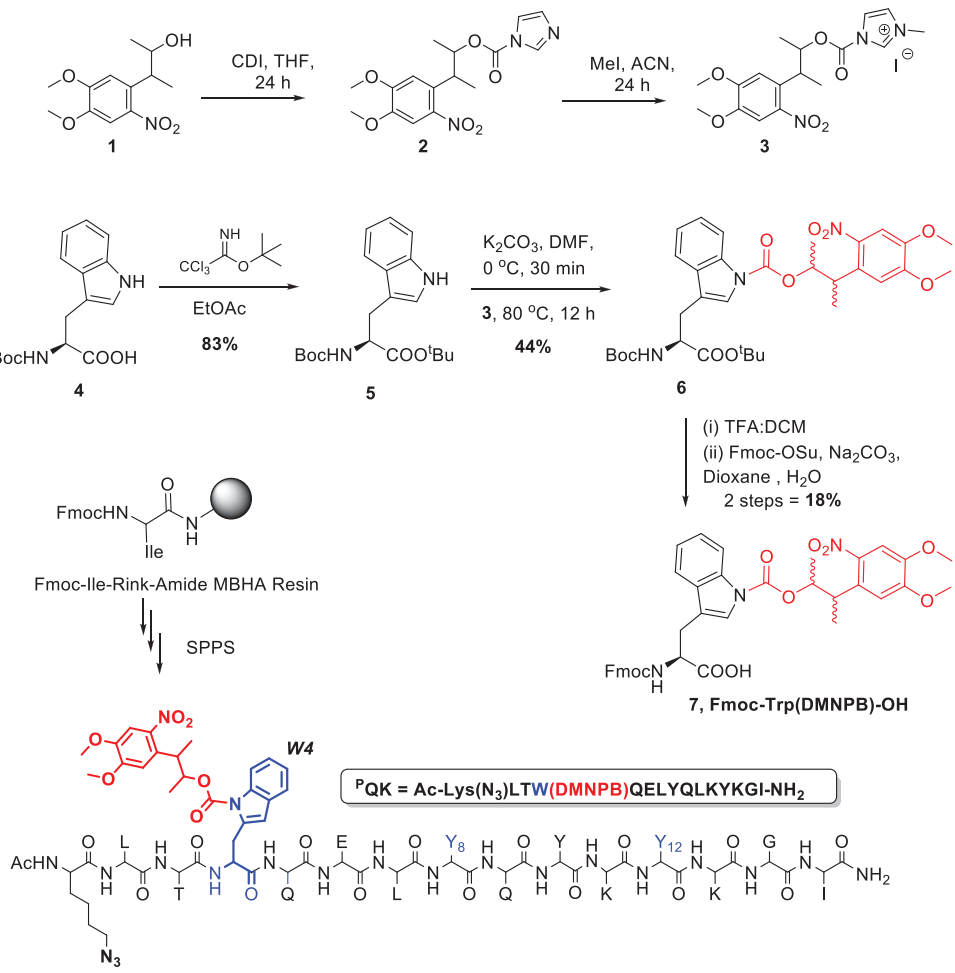

Scheme 1. Synthetic steps involved in the preparation of Fmoc-Trp(DMNPB)-OH and ^{P}QK.

a 90-fold decrease in the affinity of VEGF-15 towards VEGFR2 when Phe17 of VEGF was mutated with Ala.[3a] Based on these reported data in QK, Trp4 (W4) seemed to be the most appropriate position for introducing the photoresponsive moiety.

The photoremovable protecting group (PRPG) 3-(4,5-dimethoxy-2-nitrophenyl)butan-2-ol (DMNPB) was selected for attachment to the indole ring of Trp4 in QK. DMNPB (λ_{max} = 346 nm, λ_{max} = 4100 $M^{-1}cm^{-1}$) has been used to regulate bioactivity in cell cultures using 405 nm light with no detected photodamage.[19,21] DMNPB was attached to the aromatic amine of the indole ring via a carbamate link by following the protocol of J. A. Grzyb et al.[22] using carbamoylimidazolium salts to form carbamates from amines and alcohols (**Scheme 1**). The basic conditions (i.e., using K_2CO_3 combined with heating) needed for this reaction are not compatible with Fmoc-protection on Trp. Therefore, Boc-Trp-OH was first derivatized into Boc-Trp-O^{t}Bu[23] before reaction with the DMNPB-carbamoylimidazolium salt, to render Boc-Trp(DMNPB)-O^{t}Bu at 44% yield after column chromatography. Simultaneous Boc- and tert-butyl ester deprotection with TFA:DCM (1:1 v/v) followed by Fmoc-protection under standard conditions afforded Fmoc-Trp(DMNPB)-OH in milligrams scale and 18% yield. Synthesis protocols, characterization, and UV irradiation profile (Figure S2, Supporting Information) of Fmoc-Trp(DMNPB)-OH are detailed in the Supporting Information.

The peptide Ac-K(N_3)LTW(**DMNPB**)QELYQLKYKGI (^{P}QK) containing the DMNPB protected Trp4 was synthesized by standard Fmoc-based SPPS on Fmoc-Ile-Rink Amide MBHA resin (synthetic details in Scheme S1, Supporting Information). Coupling steps were carried out with repeating cycles of the Fmoc-protected amino acid (2 equiv.), O-(benzotriazol-1-yl)tetramethyluronium hexafluorophosphate/1-hydroxybenzotriazole (HBTU/HOBt, 2 equiv.), and diisopropylethylamine (DIPEA, 5 equiv.) at 2 h reaction time, followed by Fmoc-deprotection using 20% piperidine in DMF. The side chain of the N-terminal Lys was ^{t}Boc-protected, Glu and Thr were protected with *tert*-butyl group, and Gln with trityl-groups, respectively.

The Lys1 at the N-terminal position was substituted by the non-natural azidolysine residue (containing —N_3 group instead of —NH_2 at the ϵ-position of Lys) in order to facilitate bioorthogonal coupling of the peptide to biomaterials through a copper-free azide–alkyne cycloaddition bioorthogonal reaction with dibenzocyclooctyne (DBCO) functionalized hydrogel precursors. We anticipate, however, that other coupling strategies could also be possible and have been tested in reported work, like the introduction

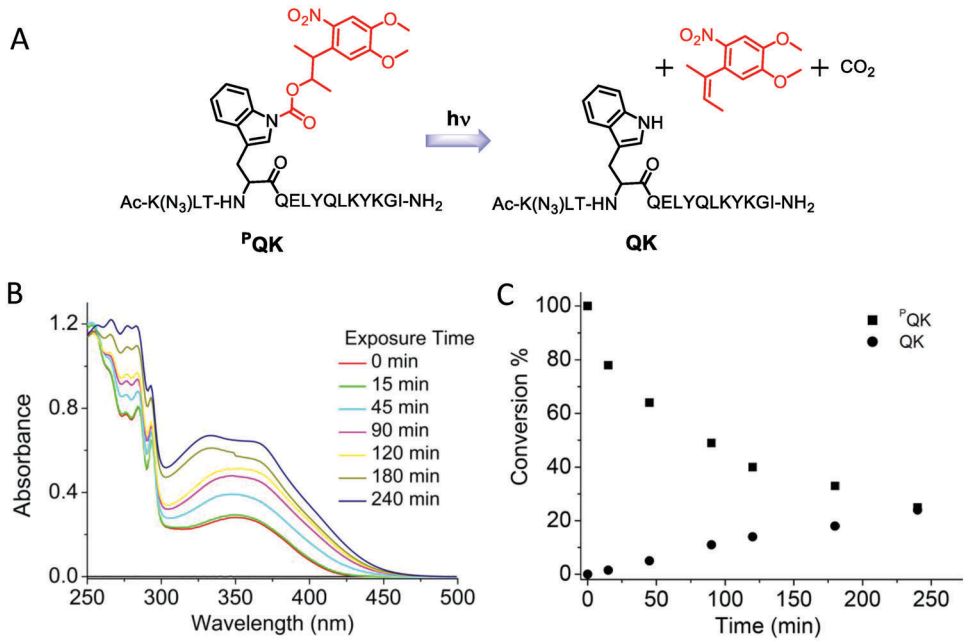

Figure 2. A) Schematic representation of photochemical activation of ^{P}QK and the expected photolysis products. B) UV–Vis spectra of a 0.25 mM solution of ^{P}QK in ACN:H_2O (1:1) after exposure at increasing time (360 nm, 1.2 mWcm^{-2}). C) Conversion (%) of ^{P}QK to QK from solution in (A), as a function of irradiation time determined by quantitative HPLC (detector 210 nm).

of a Cys residue at N-terminus,[8] additional Lysines,[11] or Acryloyl-PEG-succinimidyl ester.[10b]

The peptide Ac-Lys(N_3)LT**W(DMNPB)**QELYQLKYKGI-amide (^{P}QK) was obtained at high purity (>98%) in 5 mg scale starting from 50 mg of Fmoc-Ile-MBHA resin (loading = 0.34 mmol g^{-1}). MALDI/TOF mass spectrometry confirmed the chemical structure of the peptide. Synthesis details and corresponding spectra documenting structural characterization of the compounds are described in the Supporting Information.

2.2. Photochemical Properties of ^{P}QK

The photochemical properties of ^{P}QK were evaluated by UV spectroscopy and HPLC studies (**Figure 2**). A 0.25 mM solution of ^{P}QK in ACN:H_2O (1:1) was irradiated at 360 nm (1.2 mWcm^{-2}) at increasing exposure times (Figure 2B). Changes in the UV spectrum confirmed that photoreactions were taking place (Figure S3A, Supporting Information). HPLC elugrams (recorded in the detection channels at 210 nm) of irradiated aliquots showed a decrease in the intensity of the ^{P}QK signal (t_R = 26.2 min) and a parallel increase in the intensity of a signal at t_R = 19.9 min, which corresponded to free QK (Figure S3B, Supporting Information) according to MALDI TOF/TOF mass analysis (^{P}QK: 2259.1907 [M$^+$]; QK: 1979.1259 [M$^+$]) (Figure S3C, Supporting Information). With increasing exposure times additional signals appeared in the HPLC elugram, suggesting photochemical side reactions occurring in parallel, which couldn't be characterized. At 4 h of exposure time, 74% of ^{P}QK had been photolyzed and 24% of QK was recovered (**Figure** 2C). This value of the photochemical yield is modest compared to the yield of previously reported photoactivatable peptide cyclo(RGD(DMNPB)fC) used to guide angiogenesis with light.[19a] Ester groups, as in DMNPB-Asp, are better leaving groups than carbamates, as in DMNPB-Tryp, for this photolytic reaction[16a,24] In spite of the lower yield, preliminary experiments showed that irradiation of the ^{P}QK peptide at cell compatible doses was able to trigger angiogenesis (see next sections).

It is important to note that the irradiation conditions used in these experiments are not comparable to conditions used in the biological experiments in next sections. This is related to the fact that HPLC quantification required much low concentrations of QK (0.25 mM) and light doses for full deprotection.

2.3. Light-Triggered Angiogenesis by Photoactivation of ^{P}QK in Hydrogels

The bioactivity of ^{P}QK before and after light exposure was tested in an angiogenesis assay in a 3D cell culture. For this purpose, the star-PEG-maleimide (20 kDa) crosslinked with the di-cysteine GCRDVPMSMRGGDRCG (VPM) metalloprotease degradable peptide was used for cell encapsulation.[25] This system has been previously used in angiogenesis studies.[26] The heterobifunctional linker DBCO-PEG-SH was reacted with PEG-maleimide in a preincubation step to mediate covalent coupling of QK to PEG-maleimide by azide–alkyne cycloaddition reaction. The cell adhesive motif cyclo(RGDfC)[25a] was also coupled to the hydrogel by the thiol group of the Cys. Hydrogel precursor solutions with 4 wt% concentration of the star-PEG-maleimide, 1 mM concentrations of the peptides (QK, ^{P}QK, cyclo(RGDfC) or 1:1 mixtures of them) and 3.2 mM concentration of VPM in 10 mM HEPES buffer were used.[27] Hydrogels with initial Young's Modulus of 2.6±0.17 kPa were obtained (Table S1, Supporting Information).

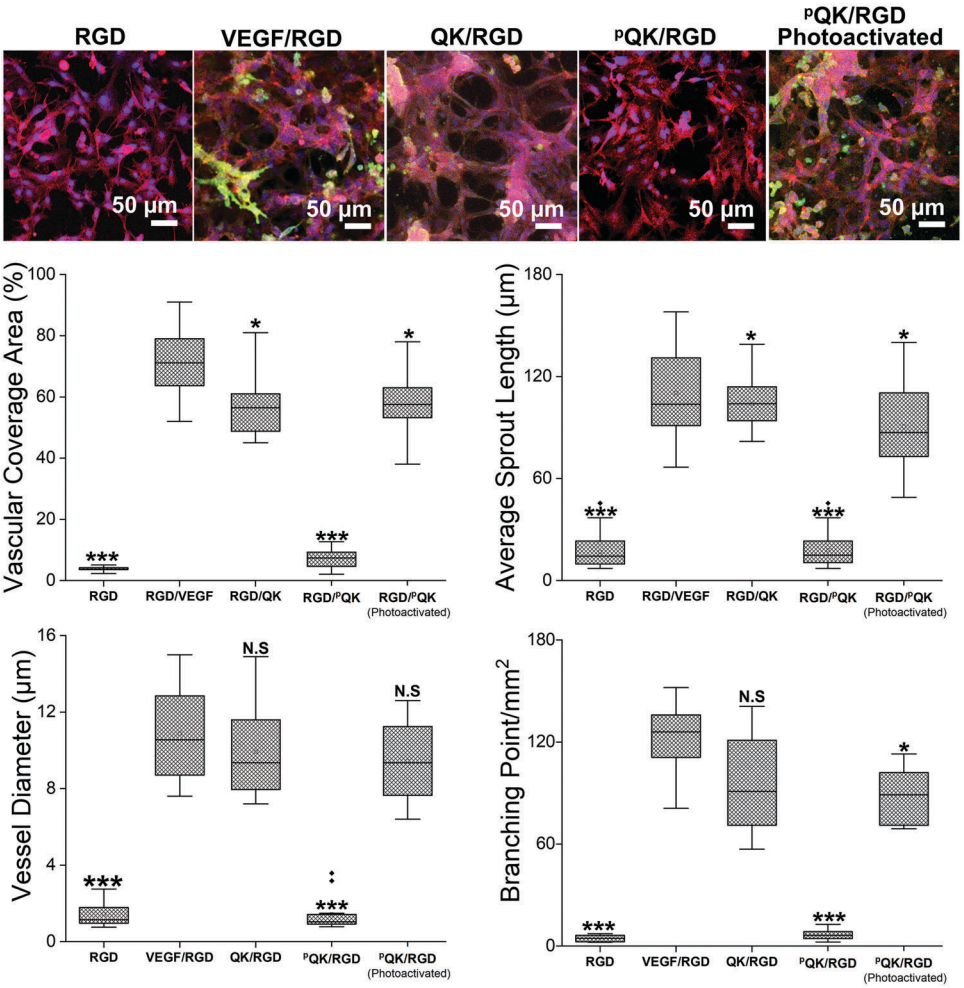

Figure 3. Confocal fluorescence microscopy images of HUVECs after 3 days of encapsulation in 3D PEG hydrogels functionalized only with the cell adhesive peptide cyclo(RGDfC) or in combination with the angiogenic molecules VEGF, QK, or ^{P}QK. The hydrogels modified with cyclo(RGDfC)/^{P}QK were irradiated at 405 nm with scanning rate of 125 µs µm^{-1} and scanned volume of 700 × 700 × 20 µm^{3}. Prior to imaging, cells were fixed and labeled with PECAM-1 antibody (green), with DAPI (blue) to stain the nucleus, and with phalloidin (red) to mark actin fibers. The graphs show the quantification of vasculogenic features and the data is represented as means ± SD from $n = 3$ independent experiments, each with at least 5 independent z-stack images. The samples were analyzed by ANOVA with a Tukey post hoc test, where statistical significance was determined between groups from $p < 0.05$ ($*p < 0.1$, $**p < 0.01$, $***p < 0.001$) and compared to control cyclo(RGDfC)/VEGF hydrogels.

Control gels modified with cyclo(RGDfC)/VEGF were also prepared in a similar way.

Human umbilical vein endothelial cells (HUVECs) were encapsulated in the hydrogels modified with different ligand combinations. Hydrogels modified with cyclo(RGDfC) promoted cell spreading and attachment, and supported viable cultures during 3 days (**Figure 3**). Hydrogels modified only with QK, ^{P}QK, or VEGF did not support cell attachment, and cells retained rounded morphology and were non-viable after 3 days of encapsulation (Figure S4, Supporting Information). Hydrogels modified with cyclo(RGDfC) in combination with QK or VEGF supported cell attachment and showed elongated tube-like morphologies with interconnected microvasculature and an ellipsoidal nuclei, as well as strong PECAM expression within 3 days of culture (Figure 3).[28] These features are indicative of the angiogenesis process and confirm the angiogenic phenotype of the RGD/QK modified PEG hydrogel, in agreement with results from other groups.[4,3b,10,29] Vasculogenic features such as vessel length and diameter, sprouting points, and vascular coverage area were quantified. Similar angiogenesis levels were found in the gels covalently modified with QK or with VEGF, indicating comparable bioactivity of the 15-mer QK or with the full protein VEGF at the concentrations used in our assay (Figure 3). RGD/QK modified hydrogels supported threefold higher cell proliferation levels than RGD modified hydrogels, which is a key indicator for enhanced vascular growth (Figure S5, Supporting Information).[30] Control experiments were performed with hydrogels covalently modified with cyclo(RGDfC) to which QK or VEGF were added in a soluble form (i.e., after gelation, not covalently bound to the hydrogel). HUVECs showed spreading, migration, and elongation also in this case, but with lower branching (twofold), sprout length (twofold), vessel diameter (twofold), and significantly lower vascular coverage area (fivefold) in comparison to gels where QK or VEGF were covalently linked to the PEG

network (Figure S6, Supporting Information). The higher activity of matrix-immobilized growth factors versus soluble growth factors has also been observed in other studies.[31] These results demonstrate that the tested gel compositions are appropriate for testing the angiogenic activity of the ^{P}QK peptide.

In hydrogels modified with cyclo(RGDfC)/^{P}QK, endothelial cells spread but showed lower vasculogenic features than in RGD/QK hydrogels during 3 days of cell culture (Figure 3). The observed morphological and vasculogenic features in cyclo(RGDfC)/^{P}QK hydrogels were similar to the control cyclo(RGDfC) hydrogels, suggesting that that ^{P}QK has no angiogenic potential due to the mutation at the Trp(4) position. Cells remained viable, indicating no inherent toxicity is associated with the photoactivatable peptide. This result confirms our hypothesis and molecular design. Introduction of the DMNPB group to the Trp(4) residue inhibits the angiogenic activity of the QK peptide.

The possibility to trigger angiogenesis in situ, that is, in the presence of cells and at selected parts of the culture, by light exposure of cyclo(RGDfC)/^{P}QK hydrogels was tested by scanning a volume of 350 × 700 ×2 0 μm^3 inside the hydrogel (200 μm below the gel surface) using a 405 nm scanning laser at increasing exposure doses between 30 and 240 μs μm^{-1}. The viability and the angiogenic activity of endothelial cells within the exposed volume were investigated after 2 days of culture and compared with the non-exposed neighboring regions. The different morphology and fate of cells inside and outside of the scanned area was clearly visible after staining (Figure S7, Supporting Information) and was confirmed by quantitative analysis. Cell viability in the exposed areas decreased from 90% to 80%, 60% and 50% after exposure from 30 to 60, 90, and 130 μs μm^{-1}, and to 80% in the non-exposed regions of the same culture. Longer exposure doses further decreased viability. These results reflect the exposure dose limits the biological experiments due to phototoxicity. Similar experiments in control hydrogels modified with cyclo(RGDfC) (i.e., no ^{P}QK) showed comparable viability values (Figure S8, Supporting Information), confirming that the drop in viability is linked to phototoxicity and not to the release of photolytic byproducts. Cells exposed at >60 μs μm^{-1} developed clear angiogenic morphological features (Figure S7, Supporting Information). The vascular area coverage after 2 days of culture continuously increased from 8% to 30%, 40%, and 63% after exposure from 30 to 60, 90, and 130 μs μm^{-1} (Figure S7, Supporting Information). Higher exposure doses (180–240 μs μm^{-1}) lead to lower values of vascular coverage area. For comparison, cells in RGD/QK hydrogels showed a vascular area coverage of 60% after 3 days (Figure 3). Cells in cyclo(RGDfC) hydrogels did not show angiogenic features irrespective of photoactivation and displayed a vascular coverage area of 6% (Figure S8, Supporting Information). These results demonstrate the possibility to trigger angiogenesis in cyclo(RGDfC)/^{P}QK hydrogels by light exposure in a site- and dose-dependent manner and are comparable to QK peptide. They also reflect that irradiation step affects cell viability and, therefore, the best possible exposure dose has to be selected attending to the two effects. Scanning conditions between 90 and 130 μs μm^{-1} were tested in our angiogenesis experiments to balance low phototoxicity and enough activated QK to trigger angiogenic response.

The photo-regulation of the angiogenic activity was further evaluated by quantifying the vascular coverage area and the branching points in hydrogels at increasing exposure doses after 3 days culture (**Figure 4**). A linear increase of the vascular area coverage (from 30% to 60%) and of the number of branching points (from 45 to 115 branched points mm^{-2}) was observed when the exposure dose increased from 50 to 125 μs μm^{-1}. The corresponding increase in PECAM expression is visible in Figure S9, Supporting Information. Higher doses did not lead to more extended angiogenesis and cells formed clumps (observable at exposure rate of 150 μs μm^{-1}), which we interpret as an indication of phototoxicity.

After optimizing the exposure conditions (i.e., 405 nm, 125 μs μm^{-1}), we induced spatially defined angiogenesis in cyclo(RGDfC)/^{P}QK hydrogels in situ by scanning a volume of 350 × 700 × 20 μm^3 inside the hydrogel (200 μm below the gel surface). Cells in the activated areas developed angiogenic features and strong PECAM expression (Figure S10, Supporting Information). Cells formed a visible microvasculature and reached a >55% vasculogenic coverage and ≈90 mm^{-2} branching points. No defined microvasculature was observed in unexposed areas after 3 days of culture (**Figure 5**).

Cells in photoactivated cyclo(RGDfC)/^{P}QK hydrogels reached angiogenic maturation within 3 days, and longer cultures (5 days) did not lead to higher levels of vascular area coverage or branching points (Figure S11, Supporting Information). HUVECs on exposed areas formed interconnected structures with vessel length, diameter, sprouting points, and vascular coverage area similar to controls with VEGF and QK (Figure 3). It should be pointed out that, according to the chemical yield of the photochemical reaction, the effective concentration of active QK in cyclo(RGDfC)/^{P}QK hydrogels after exposure should be at most 25% of the QK concentration in cyclo(RGDfC)/QK hydrogels. The comparable outcome in the angiogenesis experiment indicates that the used QK concentration is well above the saturation threshold. Reported literature reports that incorporate QK into hydrogels use a range of 0.1–0.75 mM concentration. Altogether, these results confirm that photoactivatable ^{P}QK immobilized on adhesive hydrogels allows light-driven activation of angiogenesis in gel constructs.

3. Discussion

Vascularization is a major need in biomaterials-supported tissue regeneration, and a challenge for biomaterials design.[32] VEGF is a fundamental regulator of angiogenesis and is commonly added as therapeutic molecule to promote vascularization in engineered scaffolds for tissue engineering.[20,33] As cost-efficient alternative to recombinant VEGF, the peptidomimetic QK was developed and has been successfully used to modify 3D scaffolds to promote microvascularization in 3D scaffolds in vitro and in vivo.[4,3b,29] Barbick et al. showed endothelial tubule networks on day 5 in 3D collagenase-degradable poly(ethylene glycol) diacrylate (PEGDA) modified with RGD and QK.[10] Cai et al. observed HUVECs outgrowth from spheroids on day 5 in RGD and QK modified elastin-like polypeptide hydrogels.[11] In vivo, prominent functional capillaries were observed at 21 days post-injection in QK and RGD-tethered elastin-like hydrogels.[29c] The hydrogels engineered in this article show comparable development of vessel-like structures in vitro, indicating that they contain the minimal microenvironmental requirements in terms of cell adhesive molecules

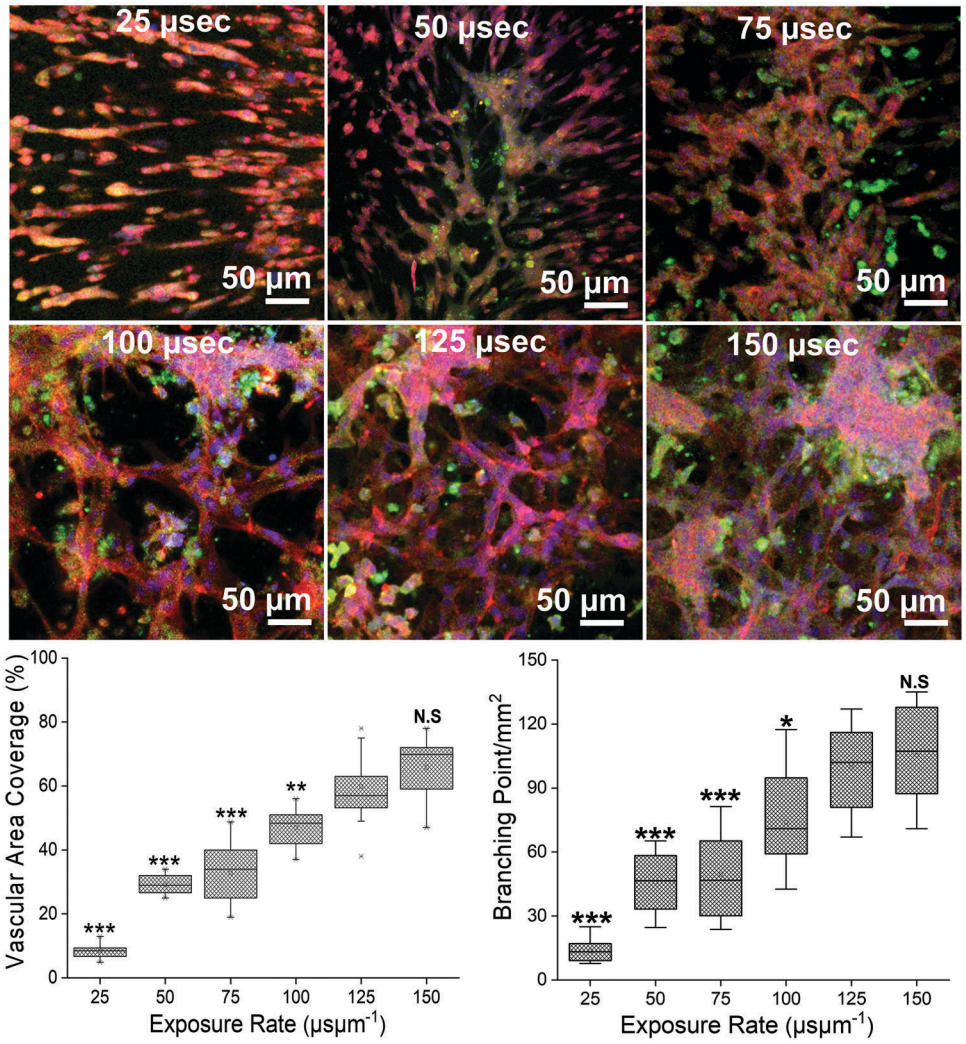

Figure 4. Confocal fluorescence microscopy images of HUVECs after 3 days of encapsulation in 3D PEG hydrogels functionalized with cyclo(RGDfC)/^{P}QK. Samples were irradiated at 405 nm with different doses by varying laser scanning rate between 25 and 150 µs µm^{-1} and with scanned volumes of 700 × 700 × 20 µm^3. Cells were labeled with PECAM-1 antibody (green), with DAPI (blue) to stain nucleus, and with phalloidin (red) to mark actin fibers. The graphs show the vascular area coverage and the number of branching points per millimeter square for the different exposure conditions and the data is represented as means ± SD from $n = 3$ independent experiments, each with at least 5 independent z-stack images. The samples were analyzed by ANOVA with a Tukey post hoc test, where statistical significance was determined between groups from $p < 0.05$ (*$p < 0.1$, **$p < 0.01$, ***$p < 0.001$) and compared to sample scanned with rate of 125 µm^{-1}.

(RGD), degradation sites (VPM), and angiogenic factors (^{P}QK) realized in an all-in-one simple 3D construct.

Several strategies have been reported to obtain hydrogels able to provide instructive signals to cells based on photosensitive molecular architectures.[34] Notable examples are the softening of PEG networks containing integrated photocleavable groups,[37b,e,35] or photoinitiated acrylate,[36] thiol-ene or oxime ligation,[34d,35] or enzymatic reactions[37] for coupling instructive ligands during cell culture at desired spaces. In contrast to these approaches, ^{P}QK involves direct incorporation of a latent, photoactivatable ligand into the 3D PEG network during gel preparation, and flexible activation at desired concentrations and spaces using light, without the need of further preparation steps.

Relevant issues in the design of angiogenic biomaterials are the controlled, sustained, and localized delivery of VEGF in combination with cell adhesive proteins.[15,29b] Reported examples do not allow spatial control of the angiogenic factor and drive vessel formation at selected sites in the regenerative niche. The photoactivatable QK, as presented in this article, can allow spatial control of the angiogenic stimulation using light to localize angiogenesis. Current approaches to obtain spatial control rely on direct patterning of endothelial cells or of depots of angiogenic factors in the scaffold, for example via bioprinting.[39] The reported approach here does not need a patterning technology to define the delivery site of the angiogenic factor. This is present in latent form all across the scaffold and can be activated with spatial resolution by simple illumination. In the past we reported spatially regulated, light-directed angiogenesis by regulating cell adhesion molecules in the presence of soluble VEGF, in vitro and in vivo.[18d,22a,c,40] In this new approach, we regulate the

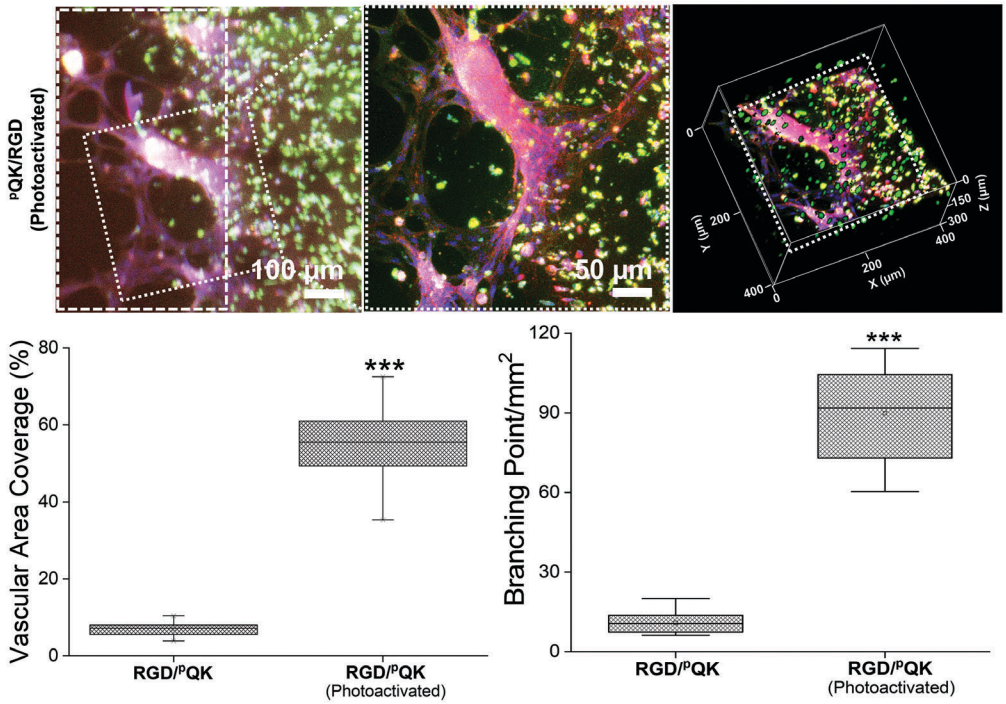

Figure 5. Confocal fluorescence microscopy images of HUVECs after 3 days of encapsulation in 3D PEG hydrogels functionalized with cyclo(RGD)fC/^{P}QK. (Left) Predefined volumes (700 × 700 × 20 µm^3) of hydrogel (marked with white dashed square) was irradiated at 405 nm with scanning rate of 125 µs µm^{-1}. Cells were labeled with PECAM-1 antibody (green), with DAPI (blue) to stain nucleus, and with phalloidin (red) to mark actin fibers. (Middle-Right) The inset of irradiated volume marked in left image with white dotted box, and corresponding Z-stack of the inset. The graphs compare the vascular area coverage and the branching points at non-irradiated and irradiated areas of the sample and the data is represented as means ± SD from $n = 5$ independent experiments, each with at least 5 independent z-stack images. The samples were analyzed by ANOVA with a Tukey–Kramer post hoc test, where statistical significance was determined between groups from $p < 0.05$ (*$p < 0.1$, **$p < 0.01$, ***$p < 0.001$) and compared to non-irradiated volumes.

concentration of the growth factor (i.e., the cue for differentiation) for the spatial control of angiogenesis without compromising cell attachment, which is a basic need for cellular viability at a days' time-scale.

Our results are promising in terms of a new functionality of the QK peptide, and validate the molecular design selected for a temporal inactivation of QK and a light-controlled spatial regulation of angiogenesis in in vitro experiments. They also show room for optimization at the photoprotecting group of the indole group of Trp, in order to improve the photochemical yield of the activation process. This is relevant for the extension of this approach to in vivo scenarios.

4. Conclusions

A photoactivable VEGF peptidomimetic, ^{P}QK, was designed and synthesized. When incorporated into degradable PEG hydrogels modified with RGD cell adhesive peptide, it allowed light-directed control of endothelial cell differentiation and angiogenesis in vitro. Regulated light exposure allowed spatial control of angiogenic differentiation of encapsulated HUVECs. These results present a new strategy to regulate blood vessel formation without the need of soluble VEGF, with the potential to be transferred into in vivo scenarios where the regulation of blood vessel formation is particularly relevant.

5. Experimental Section

Materials and Methods: 4-Arm-PEG Maleimide 20 kDa was obtained from Creative PEG work (USA), GCRDVPMSMRGGDRCG from Proteogenix (France), cyclo(RGDfC) from Peptide International (USA), VEGF was obtained from Promokine (Germany), and HEPES buffer was purchased from Sigma-Aldrich (Germany).

Cell Culture Conditions: HUVECs (Promocell) were maintained on cell culture flask coated with gelatin (0.2%). Cells were cultured in M-199 medium (Sigma, M4530) supplemented with L-glutamine (2 mM), penicillin (1000 UL^{-1}), streptomycin (100 mgL^{-1}, Sigma), ECGS (Sigma, E-2759), sodium heparin (Sigma, H-3393), and 20% fetal bovine serum (FBS, Gibco, 10270) as previously described.[19c] HUVECs were used between passages 2 to 7 were used for 3D cell culture.

Preparation and Functionalization of PEG Hydrogels for Cell Encapsulation: PEG hydrogels were prepared by adapting previously reported protocol.[25,26] Stock solutions of all components were prepared in sterile HEPES buffer (10 mM, pH 8.2) at the following concentrations: 20 kDa 4-Arm PEG maleimide (100 mg mL^{-1}, 10 wt%), cyclo(RGDfC) (3.45 mg mL^{-1}, 5 mM), QK (9.9 mg mL^{-1}, 5 mM), ^{P}QK (11.3 mg mL^{-1}, 5 mM), and VPM (26.6 mg mL^{-1}, 15.68 mM). In addition, stock solution for control sample VEGF (500 ng mL^{-1}) was prepared in PBS (pH 7.4).

In the case of QK/^{P}QK functionalized hydrogels, 4-Arm-PEG maleimide solution (5 µL, 10 wt%) was preincubated for 5 min at 37 °C with the bifunctional linker DBCO-PEG-SH (0.5 µL, 10 mM in HEPES) and then incubated for a further 25 min with QK/^{P}QK stock solutions as described below.

Monofunctionalized hydrogels were prepared by mixing 4-Arm-PEG maleimide solution (4 µL, 10 wt%) with either cyclo(RGDfC) (2 µL, 5 mM),

VEGF (1 µL, 500 ng mL^{-1}, PBS), QK (2 µL, 5 mM), or ^{P}QK (2 µL, 5 mM) and incubated for 30 min at 37 °C. Bifunctionalized hydrogels with combination of cyclo(RGDfC) either with VEGF (500 ng mL^{-1}), QK, or ^{P}QK (5 mM) solutions was prepared by mixing 1.5 µL from each solution with 4-Arm-PEG maleimide solution (5 µL, 10 wt%), followed by incubation for 30 min at 37 °C.

HUVECs (3×10^7 mL^{-1}) were suspended in above solutions and added to each well (8 µL) of Ibidi 15-μwell angiogenesis slide. VPM (2 µL, 15.6 mM) was immediately added to cell suspended solution to quickly initiate (within 30 sec–1 min) gelation and avoid sedimentation of cells. Gels were allowed to polymerize for further 15 min at 37 °C, followed by addition of media (50 µL) to each well. Cells were cultured in 3D hydrogels for further 24–96 h at 37 °C and 5% CO_2, with fresh medium exchange every day.

Photo-Activation in 3D: Cell encapsulated hydrogels modified with ^{P}QK were exposed by using laser (λ = 405 nm, intensity = 85%) from Zeiss 880 LSM microscope equipped with incubation chamber (37 °C and 5% CO_2). Scanning speed of laser was tuned between 25–240 µs µm^{-1} in combination with 10xEC Plan Neofluar (NA 0.3) objective. The predefined volume patterns were drawn by using Zeiss LSM 880 ROI tool. After, exposure cell culture medium was replaced with fresh medium within 30 min in order to remove the photocleaved byproduct. The samples were later kept either in a cell culture incubator or observed with bright field imaging.

Cell Viability Assay: Cell culture media was removed and hydrogels were incubated for 5 min with fluorescein diacetate (40 µg mL^{-1}, Sigma, F7378) and propidium iodide (30 µg mL^{-1}, Sigma, P4170) solution in PBS. Samples were washed twice with PBS and immediately imaged with a Zeiss LSM 880 confocal microscope at 10× magnification using excitation wavelengths of 488 and 543 nm. The z-stack fluorescence microscopy images were captured with the Zen Black software (version 2.1) and live (green) and dead (red) cells were counted manually in each slice (4 µm) of z-stack to calculate the percentage viability of each sample. For each sample at least five independent z-stacks were analyzed (≈300–1400 cells per samples).

Proliferation and Angiogenesis Assay: Hydrogels were fixed with 4% aqueous PFA solution for 2 h, washed with PBS and blocked with 1% BSA solution for 1 h. Cells were permeabilized with 0.5% Triton X-100 for 1 h and incubated with monoclonal goat anti-rabbit PECAM-1 primary antibody (1:50 in 1% BSA for, Abcam) 1 h and washed with PBS. Hydrogels were incubated with anti-rabbit Alexa flour-488 secondary antibody (1:400 in water, Thermo Fisher Scientific) for 5 h. Subsequently, cells were washed with PBS and nuclei were stained with DAPI (1:500 in water, Life Technology) and actin fibers were labelled with TRITC-phalloidin (1:200 in water, Thermo Fisher Scientific). Samples were washed twice with PBS and imaged with a Zeiss LSM 880 confocal microscope at 10× magnification using excitation wavelengths of 405, 488, and 543 nm. The z-stack fluorescence microscopy images were captured with the Zen Black software (version 2.1) and nuclei (blue) were counted manually in each slice (4 µm) of z-stack to calculate the number of cells in each sample for quantification of cell proliferation. For each sample at least five independent z-stacks were analyzed (≈400–1200 cells per samples) to calculate cell proliferation. Vasculogenic features (i.e., vascular coverage area, vessel diameter, average sprout length, and branching points) were quantified automatically from a whole z-stack image by using the angiogenesis analyzer tool (http://image.bio.methods.free.fr/ImageJ/?Angiogenesis-Analyzer-for-ImageJ&artpage=3-6) in ImageJ software (version 2.0).

General Statistical Analysis: The data are expressed as the mean ± standard deviation and presented without further pre-processing. All experiments comprised of at least two independent experimental batches performed under identical conditions. Statistical analysis for parametric results was performed by one-way ANOVA with a Tukey–Kramer post hoc test of the variance using Origin software (version 2020). In all cases, statistical significance was determined between groups using a value of $p < 0.05$ ($^{*}p < 0.1$, $^{**}p < 0.01$, $^{***}p < 0.001$) and compared against respective controls.

Supporting Information

Supporting Information is available from the Wiley Online Library or from the author.

Acknowledgements

R.V.N. and A.F. contributed equally to this work. All authors contributed to the design of the experiments, discussions and writing of the paper. R.V.N. and A.F. contributed equally to the experimental work. R.V.N. carried out the synthetic and photochemical studies and A.F. performed the biological experiments.

Open access funding enabled and organized by Projekt DEAL.

Conflict of Interest

The authors declare no conflict of interest.

Data Availability Statement

Research data are not shared.

Keywords

light regulated angiogenesis, photoactivatable peptides, photoactivatable QK, photocaged tryptophan, photoresponsive hydrogels

Received: March 14, 2021
Revised: May 6, 2021
Published online:

[1] a) M. Potente, H. Gerhardt, P. Carmeliet, *Cell* **2011**, *146*, 873; b) P. S. Briquez, L. E. Clegg, M. M. Martino, F. M. Gabhann, J. A. Hubbell, *Nat. Rev. Mater.* **2016**, *1*, 15006; c) E. A. Silva, D. J. Mooney, *J. Thromb. Haemostasis* **2007**, *5*, 590.

[2] P. Vempati, A. S. Popel, F. M. Gabhann, *Cytokine Growth Factor Rev.* **2014**, *25*, 1.

[3] a) L. D. D'Andrea, G. Iaccarino, R. Fattorusso, D. Sorriento, C. Carannante, D. Capasso, B. Trimarco, C. Pedone, *Proc. Natl. Acad. Sci. U. S. A.* **2005**, *102*, 14215; b) L. D. D'Andrea, L. De Rosa, C. Vigliotti, M. Cataldi, *New Horiz. Transl. Med.* **2017**, *3*, 233; c) D. Diana, A. Basile, L. De Rosa, R. Di Stasi, S. Auriemma, C. Arra, C. Pedone, M. C. Turco, R. Fattorusso, L. D. D'Andrea, *J. Biol. Chem.* **2011**, *286*, 41680; d) L. De Rosa, F. Finetti, D. Diana, R. Di Stasi, S. Auriemma, A. Romanelli, R. Fattorusso, M. Ziche, L. Morbidelli, L. D. D'Andrea, *Sci. Rep.* **2016**, *6*, 31295; e) D. Capasso, S. Di Gaetano, V. Celentano, D. Diana, L. Festa, R. Di Stasi, L. De Rosa, R. Fattorusso, L. D. D'Andrea, *Mol. BioSyst.* **2017**, *13*, 1619; f) L. Wang, P. Coric, S. Broussy, R. Di Stasi, L. Zhou, L. D. D'Andrea, L. Ji, M. Vidal, S. Bouaziz, W.-Q. Liu, *Eur. J. Med. Chem.* **2019**, *169*, 65.

[4] F. Finetti, A. Basile, D. Capasso, S. Di Gaetano, R. Di Stasi, M. Pascale, C. M. Turco, M. Ziche, L. Morbidelli, L. D. D'Andrea, *Biochem. Pharmacol.* **2012**, *84*, 303.

[5] a) G. Santulli, M. Ciccarelli, G. Palumbo, A. Campanile, G. Galasso, B. Ziaco, G. G. Altobelli, V. Cimini, F. Piscione, L. D. D'Andrea, C. Pedone, B. Trimarco, G. Iaccarino, *J. Transl. Med.* **2009**, *7*, 41; b) G. Pignataro, B. Ziaco, A. Tortiglione, R. Gala, O. Cuomo, A. Vinciguerra,

D. Lapi, T. Mastantuono, S. Anzilotti, L. D. D'Andrea, C. Pedone, G. di Renzo, L. Annunziato, M. Cataldi, *ACS Chem. Neurosci.* **2015**, *6*, 1517; c) A. Verheyen, E. Peeraer, D. Lambrechts, K. Poesen, P. Carmeliet, M. Shibuya, I. Pintelon, J. P. Timmermans, R. Nuydens, T. Meert, *Neuroscience* **2013**, *244*, 77.

[6] V. A. Kumar, N. L. Taylor, S. Shi, B. K. Wang, A. A. Jalan, M. K. Kang, N. C. Wickremasinghe, J. D. Hartgerink, *ACS Nano* **2015**, *9*, 860.

[7] a) W. Mulyasasmita, L. Cai, Y. Hori, S. C. Heilshorn, *Tissue Eng., Part A* **2014**, *20*, 2102; b) M. J. Webber, J. Tongers, C. J. Newcomb, K. T. Marquardt, J. Bauersachs, D. W. Losordo, S. I. Stupp, *Proc. Natl. Acad. Sci. U. S. A.* **2011**, *108*, 13438.

[8] Y. Yang, Q. Yang, F. Zhou, Y. Zhao, X. Jia, X. Yuan, Y. Fan, *J. Mater. Sci.: Mater. Med.* **2016**, *27*, 106.

[9] C. Y. Lin, Y. R. Wang, C. W. Lin, S. W. Wang, H. W. Chien, N. C. Cheng, W. B. Tsai, J. Yu, *BioResearch* **2014**, *3*, 297.

[10] a) E. A. Phelps, K. L. Templeman, P. M. Thulé, A. J. García, *Drug Delivery Transl. Res.* **2015**, *5*, 125; b) J. E. Leslie-Barbick, J. E. Saik, D. J. Gould, M. E. Dickinson, J. L. West, *Biomaterials* **2011**, *32*, 5782.

[11] L. Cai, C. B. Dinh, S. C. Heilshorn, *Biomater. Sci.* **2014**, *2*, 757.

[12] T. R. Chan, P. J. Stahl, S. M. Yu, *Adv. Funct. Mater.* **2011**, *21*, 4252.

[13] L. Wang, M. Zhao, S. Li, U. J. Erasquin, H. Wang, L. Ren, C. Chen, Y. Wang, C. Cai, *ACS Appl. Mater. Interfaces* **2014**, *6*, 8401.

[14] A. Uccelli, T. Wolff, P. Valente, N. Di Maggio, M. Pellegrino, L. Gurke, A. Banfi, R. Gianni-Barrera, *Swiss Med. Wkly.* **2019**, *149*, w20011.

[15] S. M. Anderson, S. N. Siegman, T. Segura, *Biomaterials* **2011**, *32*, 7432.

[16] a) P. Klán, T. Šolomek, C. G. Bochet, A. Blanc, R. Givens, M. Rubina, V. Popik, A. Kostikov, J. Wirz, *Chem. Rev.* **2012**, *113*, 119; b) G. Mayer, A. Heckel, *Angew. Chem., Int. Ed. Engl.* **2006**, *45*, 4900; c) V. n. San Miguel, C. G. Bochet, A. del Campo, *J. Am. Chem. Soc.* **2011**, *133*, 5380.

[17] a) D. L. Alge, K. S. Anseth, *Nat. Mater.* **2013**, *12*, 950; b) C. Bao, L. Zhu, Q. Lin, H. Tian, *Adv. Mater.* **2015**, *27*, 1647; c) G. Huang, F. Li, X. Zhao, Y. Ma, Y. Li, M. Lin, G. Jin, T. J. Lu, G. M. Genin, F. Xu, *Chem. Rev.* **2017**, *117*, 12764.

[18] a) D. D. Young, A. Deiters, *Org. Biomol. Chem.* **2007**, *5*, 999; b) J. E. T. Corrie, T. Furuta, R. Givens, A. L. Yousef, M. Goeldner, in *Dynamic Studies in Biology: Phototriggers, Photoswitches and Caged Biomolecules*, Wiley-VCH Verlag GmbH & Co. KGaA, Weinheim, Germany **2005**, pp. 1; c) A. Specht, F. Bolze, Z. Omran, J. F. Nicoud, M. Goeldner, *HFSP J.* **2009**, *3*, 255; d) A. Farrukh, J. I. Paez, A. del Campo, *Adv. Funct. Mater.* **2019**, *29*, 1807734; e) S. Pradhan, O. A. Banda, C. J. Farino, J. L. Sperduto, K. A. Keller, R. Taitano, J. H. Slater, *Adv. Healthcare Mater.* **2020**, *9*, 1901255.

[19] a) S. Petersen, J. M. Alonso, A. Specht, P. Duodu, M. Goeldner, A. del Campo, *Angew. Chem., Int. Ed.* **2008**, *47*, 3192; b) T. T. Lee, J. R. García, J. I. Paez, A. Singh, E. A. Phelps, S. Weis, Z. Shafiq, A. Shekaran, A. del Campo, A. J. García, *Nat. Mater.* **2014**, *14*, 352; c) M. J. Salierno, A. J. García, A. del Campo, *Adv. Funct. Mater.* **2013**, *23*, 5974; d) M. Wirkner, J. M. Alonso, V. Maus, M. Salierno, T. T. Lee, A. J. García, A. del Campo, *Adv. Mater.* **2011**, *23*, 3907; e) R. V. Nair, A. Farrukh, A. Del Campo, *ChemBioChem* **2018**, *19*, 1280; f) A. Farrukh, W. Fan, S. Zhao, M. Salierno, J. I. Paez, A. Del Campo, *ChemBioChem* **2018**, *19*, 1271.

[20] R. Di Stasi, D. Diana, D. Capasso, S. Di Gaetano, L. De Rosa, V. Celentano, C. Isernia, R. Fattorusso, L. D. D'Andrea, *Chem. - Eur. J.* **2018**, *24*, 11461.

[21] a) Y. Zheng, A. Farrukh, A. Del Campo, *Langmuir* **2018**, *34*, 14459; b) T. T. Lee, J. R. Garcia, J. I. Paez, A. Singh, E. A. Phelps, S. Weis, Z. Shafiq, A. Shekaran, A. Del Campo, A. J. Garcia, *Nat. Mater.* **2015**, *14*, 352.

[22] J. A. Grzyb, M. Shen, C. Yoshina-Ishii, W. Chi, R. S. Brown, R. A. Batey, *Tetrahedron* **2005**, *61*, 7153.

[23] J. Thierry, C. Yue, P. Potier, *Tetrahedron Lett.* **1998**, *39*, 1557.

[24] L. Kammari, L. Plistil, J. Wirz, P. Klan, *Photochem. Photobiol. Sci.* **2007**, *6*, 50.

[25] a) E. A. Phelps, N. O. Enemchukwu, V. F. Fiore, J. C. Sy, N. Murthy, T. A. Sulchek, T. H. Barker, A. J. García, *Adv. Mater.* **2012**, *24*, 64; b) B. H. Northrop, S. H. Frayne, U. Choudhary, *Polym. Chem.* **2015**, *6*, 3415.

[26] A. Farrukh, J. I. Paez, A. del Campo, *Adv. Funct. Mater.* **2019**, *29*, 1807734.

[27] K. Chwalek, K. R. Levental, M. V. Tsurkan, A. Zieris, U. Freudenberg, C. Werner, *Biomaterials* **2011**, *32*, 9649.

[28] G. Cao, C. D. O'Brien, Z. Zhou, S. M. Sanders, J. N. Greenbaum, A. Makrigiannakis, H. M. DeLisser, *Am. J. Physiol.: Cell Physiol.* **2002**, *282*, C1181.

[29] a) L. D. D'Andrea, G. Iaccarino, R. Fattorusso, D. Sorriento, C. Carannante, D. Capasso, B. Trimarco, C. Pedone, *Proc. Natl. Acad. Sci. U. S. A.* **2005**, *102*, 14215; b) A. H. Van Hove, D. S. Benoit, *Front. Bioeng. Biotechnol.* **2015**, *3*, 102; c) T. Flora, I. G. de Torre, M. Alonso, J. C. Rodríguez-Cabello, *J. Mater. Sci.: Mater. Med.* **2019**, *30*, 30.

[30] K.-A. Norton, A. S. Popel, *Sci. Rep.* **2016**, *6*, 36992.

[31] V. Moulisová, C. Gonzalez-García, M. Cantini, A. Rodrigo-Navarro, J. Weaver, M. Costell, R. S. i Serra, M. J. Dalby, A. J. García, M. Salmerón-Sánchez, *Biomaterials* **2017**, *126*, 61.

[32] V. Mastrullo, W. Cathery, E. Velliou, P. Madeddu, P. Campagnolo, *Front. Bioeng. Biotechnol.* **2020**, *8*, 188.

[33] G. Papavasiliou, M. H. Cheng, E. M. Brey, *J. Invest. Med.* **2010**, *58*, 838.

[34] a) B.-h. Chueh, Y. Zheng, Y.-s. Torisawa, A. Y. Hsiao, C. Ge, S. Hsiong, N. Huebsch, R. Franceschi, D. J. Mooney, S. Takayama, *Biomed. Microdevices* **2010**, *12*, 145; b) M. A. Azagarsamy, I. A. Marozas, S. Spaans, K. S. Anseth, *ACS Macro Lett.* **2015**, *5*, 19; c) R. Y. Tam, L. J. Smith, M. S. Shoichet, *Acc. Chem. Res.* **2017**, *50*, 703; d) C. A. DeForest, D. A. Tirrell, *Nat. Mater.* **2015**, *14*, 523; e) C. A. DeForest, K. S. Anseth, *Nat. Chem.* **2011**, *3*, 925; f) A. M. Kloxin, K. J. Lewis, C. A. DeForest, G. Seedorf, M. W. Tibbitt, V. Balasubramaniam, K. S. Anseth, *Integr. Biol.* **2012**, *4*, 1540; g) D. L. Alge, K. S. Anseth, *Nat. Mater.* **2013**, *12*, 950; h) T. E. Brown, K. S. Anseth, *Chem. Soc. Rev.* **2017**, *46*, 6532.

[35] C. A. DeForest, K. S. Anseth, *Angew. Chem.* **2012**, *124*, 1852.

[36] S.-H. Lee, J. J. Moon, J. L. West, *Biomaterials* **2008**, *29*, 2962.

[37] K. A. Mosiewicz, L. Kolb, A. J. van der Vlies, M. M. Martino, P. S. Lienemann, J. A. Hubbell, M. Ehrbar, M. P. Lutolf, *Nat. Mater.* **2013**, *12*, 1072.

[38] a) N. W. Pensa, A. S. Curry, M. S. Reddy, S. L. Bellis, *J. Biomed. Mater. Res., Part A* **2019**, *107*, 2764; b) N. W. Pensa, A. S. Curry, M. S. Reddy, S. L. Bellis, *PLoS One* **2019**, *14*, e0213592.

[39] M. D. Sarker, S. Naghieh, N. K. Sharma, X. Chen, *J. Pharm. Anal.* **2018**, *8*, 277.

[40] M. Wirkner, S. Weis, V. San Miguel, M. Álvarez, R. A. Gropeanu, M. Salierno, A. Sartoris, R. E. Unger, C. J. Kirkpatrick, A. del Campo, *ChemBioChem* **2011**, *12*, 2623.